第 31 卷第 9 期
2015 年 9 月

无 机 化 学 学 报
CHINESE JOURNAL OF INORGANIC CHEMISTRY

Vol.31 No.9
1867-1874

基于四甲基取代六元瓜环的四核稀土镝簇合物的慢磁弛豫

陈文建 孔祥建* 龙腊生* 郑兰荪

(固体表面物理化学国家重点实验室,厦门大学化学化工学院化学系,厦门 361005)

摘要: 报道了 2 个基于四甲基取代六元瓜环的三明治型四核稀土簇合物,$[Ln_4(\mu_3\text{-}OH)_4(\mu_2\text{-}OH)_2(H_2O)_4(NO_3)_2(TMeQ[6])_2]\cdot(NO_3)_4\cdot 26H_2O$(Ln=Dy,**1**;Ln=Tb, **2**)。晶体结构分析显示 2 个簇合物包含 2 个四甲基取代瓜环夹心的四核稀土立方烷结构,$[Ln_4(\mu_3\text{-}OH)_4]^{8+}$。磁性研究显示化合物 **1** 显示了慢磁弛豫行为。由于六元瓜环配体可以有效的传递能量给稀土铽离子,化合物 **2** 具有较好的发光性能。

关键词: 簇合物; 磁性; 发光; 六元瓜环
中图分类号: O614.342 **文献标识码**:A **文章编号**: 1001-4861(2015)09-1867-08
DOI:10.11862/CJIC.2015.226

Slow Magnetic Relaxation in Sandwich-Type Tetranuclear Dysprosium Complex with TMeQ[6] (TMeQ[6]=*α*, *α*, *δ*, *δ*-Tetramethylcucurbit[6]uril)

CHEN Wen-Jian KONG Xiang-Jian* LONG La-Sheng* ZHENG Lan-Sun

(*State Key Laboratory of Physical Chemistry of Solid Surface and Department of Chemistry, College of Chemistry and Chemical Engineering, Xiamen University, Xiamen, Fujian* 361005, *China*)

Abstract: Two TMeQ[6]-supported sandwich tetranuclear complexes, $[Ln_4(\mu_3\text{-}OH)_4(\mu_2\text{-}OH)_2(H_2O)_4(NO_3)_2(TMeQ[6])_2](NO_3)_4\cdot 26H_2O$ (Ln=Dy, **1**; Ln=Tb, **2**), have been prepared and characterized. Crystal structural analysis reveals that both complexes contain a cubane-like $[Ln_4(\mu_3\text{-}OH)_4]^{8+}$ cluster core sandwiched between two TMeQ[6] macrocycles. Magnetic investigations indicate that complex **1** displays slow magnetization relaxation. Complex **2** exhibits intense photoluminescence owing to the efficient energy transfer from TMeQ[6] ligand to Tb^{3+} ion. CCDC: 929607, **1**; 929608, **2**.

Key words: cluster; magnetism; photoluminescence; curcurbit[6]

0 Introduction

Single-molecule magnets (SMMs) continue to be an inviting research field in recent decades, not only because of their intriguing properties, but also their potential applications in quantum computing[1], magnetic information storage [2], nanoelectrons [3], and molecular spintronics[4-5]. Since the first SMM of $[Mn_{12}O_{12}(AcO)_{16}(H_2O)_4]$ appearance in the early 1990s[6], a large number of transition-metal polynuclear compounds with SMMs property have been reported.

It was found that high spin lanthanide ions are good candidates for constructing new SMMs, due to their large intrinsic magnetic anisotropy[8-11]. However, because of the synthetic challenges and the difficulty in promoting magnetic interactions via connecting by bridging ligands, rational design and assembly of pure lanthanide based SMMs remain a challenge[9-11]. Investigations on the lanthanide cluster-based molecular magnetism suggest that selecting appropriate bridging

收稿日期:2015-06-01。收修改稿日期:2015-07-07。
国家自然科学基金 (nos.21422106, 21371144, 21431005)资助项目。
*通讯联系人。E-mail:xjkong@xmu.edu.cn; lslong@xmu.edu.cn;会员登记号:S06N455S1203(陈文建);S06N3944M1007(龙腊生)。

ligand is crucial to the construction of pure lanthanide -based SMMs. So far, a number of organic ligands, such as aminoacids [11-12], *o*-vanillin [8b], Schiff bases[13], carboxylates[14], β-diketones[15], and calixarenes[9,16] have been used to construct lanthanide SMMs, among which Schiff base based on *o*-vanillin[8b,10b,17] has been most studied.

Cucurbit[*n*]urils (Q[*n*]s, Fig.1a) and their alkyl-substituted derivatives have proved to be an excellent class of both ligands and organic building blocks due to the two opening portals of these macrocycles with its unique cavity rimmed with π-rich dipole carbonyl groups[18-21]. Although a large number of Q[*n*]s supported transition metal-containing[22] and lanthanide-containing coordination compounds have been reported[23], Q[*n*]s supported polynuclear lanthanide SMMs are rare [24]. Herein we report a TMeQ [6] (Fig.1b) supported Dy_4 cluster complex, formulated as $[Dy_4(\mu_3\text{-}OH)_4(\mu_2\text{-}OH)_2(H_2O)_4(NO_3)_2(TMeQ[6])_2]\cdot(NO_3)_4\cdot 26H_2O$ (**1**), which features a disordered $[Dy_4(\mu_3\text{-}OH)_4]^{8+}$ cubane cluster core sandwiched by two TMeQ [6] macrocycles. Alternating current susceptibility measurements reveal that the compound **1** exhibits slow relaxation of magnetization. To the best of our knowledge, this is the first example of a TMeQ[6] supported lanthanide cluster with slow relaxation of magnetization. We also obtain its Tb^{3+} analogue $[Tb_4(\mu_3\text{-}OH)_4(\mu_2\text{-}OH)_2(H_2O)_4(NO_3)_2(TMeQ[6])_2](NO_3)_4\cdot 26H_2O$ (**2**), which exhibits interesting luminescent property.

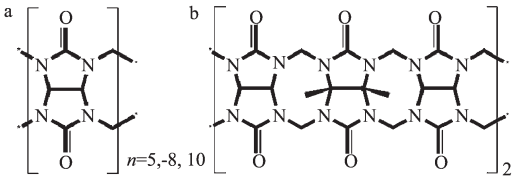

Fig.1 Molecular structure of Q[*n*]s (a) and TMeQ[6] (b)

1 Experimental

1.1 Materials and methods

All reagents were of commercial origin with 99% purity and were used as received. TMeQ [6] was prepared by procedures reported elsewhere[19e]. The C, H and N microanalyses were carried out with a CE instruments EA 1110 elemental analyzer. TGA curve was obtained on a SDT Q600 thermal analyzer. Magnetic susceptibility was measured by a Quantum Design MPMS superconducting quantum interference device (SQUID).

1.2 Synthesis

1.2.1 $[Dy_4(\mu_3\text{-}OH)_4(\mu_2\text{-}OH)_2(H_2O)_4(NO_3)_2(TMeQ[6])_2](NO_3)_4\cdot 26H_2O$ (**1**)

TMeQ[6] (0.138 g, 0.125 mmol), $Dy(NO_3)_3\cdot 5H_2O$ (0.484 g, 1.00 mmol) and 1*H*-[3-(4-pyridyl)pyrazole]-acetic acid (0.104 g, 0.50 mmol) were dissolved in 40.0 mL of water while stirring at 70 ℃. The mixture was heated to 100 ℃ and refluxed for 2 h. The filtrate was left to stand at room temperature in an open beaker (50 mL). After six days, colorless crystals of **1** were obtained and collected in a yield of 36% on the basis of TMeQ[6]. Anal. Calcd. for **1**(%): C, 25.48; H, 4.12; N, 20.06. Found (%): C, 25.58; H, 4.22; N, 20.12.

1.2.2 $[Tb_4(\mu_3\text{-}OH)_4(\mu_2\text{-}OH)_2(H_2O)_4(NO_3)_2(TMeQ[6])_2](NO_3)_4\cdot 26H_2O$ (**2**)

This compound was prepared using the same procedure as described above for the synthesis of its Dy cognate, but using 0.481 g $Tb(NO_3)_3\cdot 5H_2O$ (1.00 mmol) instead of $Dy(NO_3)_3\cdot 5H_2O$. Colorless crystals of **2** were obtained after a week and collected in a yield of 40% on the basis of TMeQ[6]. Anal. Calcd. for **2** (%): C, 25.58; H, 4.13; N, 20.14. Found(%): C, 25.66; H, 4.20; N, 20.22.

1.2.3 Single-Crystal X-ray structure determination

Data collections were performed on a Bruker Apex-2000 diffractometer using graphite monochromated Mo $K\alpha$ radiation (λ=0.071 073 nm) at 173 K. Absorption corrections were applied using the ultiscan program SADABS [25]. The structures were solved by indirect methods(SHELXTL Version 5.10)[25]. Non-hydrogen atoms were refined anisotropically by full-matrix least-squares method on F^2. The hydrogen atoms of the organic ligand were generated geometrically (C-H, 0.096 nm). Because of severe disorder, 21 water molecules and $3NO_3^-$ in the unit cell have been taken into account by the SQUEEZE. Details of the crystal parameters, data collection conditions and refinement parameters for compounds **1** and **2** are

Table 1　Crystal Data and Structure Refinement Details for Compounds 1 and 2

Compound	**1**	**2**
Empirical formula	$C_{80}H_{154}N_{54}O_{78}Dy_4$	$C_{80}H_{154}N_{54}O_{78}Tb_4$
Formula weight	3 770.39	3 756.07
Crystal system	Triclinic	Triclinic
Space group	$P\bar{1}$	$P\bar{1}$
a / nm	1.497 4(1)	1.537 7(3)
b / nm	1.923 5(1)	1.915 4(4)
c / nm	2.434 3(1)	2.444 9(5)
α / (°)	86.303(3)	87.136(3)
β / (°)	85.516(3)	86.448(4)
γ / (°)	67.176(4)	66.428(3)
V / nm	6.438(1)	6.585(2)
Z	2	2
D_c / (g·cm^{-3})	1.641	1.590
T / K	173(2)	173(2)
μ / mm^{-1}	2.396	2.220
Reflections / unique	22 573	22 904
Reflections / observed	13 934	16 794
Parameters	1 825	1 767
R_{int}	0.064 8	0.042 1
R [$I>2\sigma(I)$][a]	0.092 9	0.048 7
wR [$I>2\sigma(I)$][b]	0.239 4	0.124 3
R (all data)	0.133 4	0.064 2
wR (all data)	0.261 3	0.130 8
GOF on F^2	1.079	0.998

[a] $R_1=\sum||F_o|-|F_c||/\sum|F_o|$; [b] $wR_2=\{\sum[w(F_o^2-F_c^2)^2]/\sum[w(F_o^2)^2]\}^{1/2}$

summarized in Table 1.

CCDC: 929607, **1**; 929608, **2**.

2　Results and discussion

2.1　Synthesis

The reaction of TMeQ[6], $Ln(NO_3)_3$, and 1*H*-[3-(4-pyridyl)pyrazole]-acetic acid (1∶8∶4) in distilled water produces **1** (Ln=Dy) or **2** (Ln=Tb) in good yields. Originally, we intent to synthesize rare-earth-metal coordination polymers that conatin 1*H*-[3-(4-pyridyl) pyrazole]acetic acid ligand and TMeQ [6]. However, the experimental results show that 1*H*-[3-(4-pyridyl) pyrazole]-acetic acid is not coordinated with rare earth ions in complexes **1** and **2**. The ligand of 1*H*-[3-(4-pyridyl)pyrazole]-acetic acid is necessary for the reactions, although it is not incorporated into the structures of **1** and **2**. Absence of 1*H*-[3-(4-pyridyl) pyrazole]-acetic acid would result in the formation of an one-dimensional chain comprising TMeQ[6] molecules and $[Ln(H_2O)_8]^{3+}$ with a 1∶1 ratio through hydrogen bonding (Fig.S1). The ligand may play the role of controlling the hydrolysis of the rare earth ions to limit the degree of aggregation of the hydroxo intermediates.

2.2　Description of crystal structures

Complexes **1** and **2** are isomorphous, so only the structure of **1** is described in detail. X-ray Single-crystal structure analysis reveals that complex **1** crystallizes in triclinic, $P\bar{1}$ space group. As shown in Fig.2, complex **1** possesses a sandwich structure of $[Dy_4(\mu_3\text{-}OH)_4(\mu_2\text{-}OH)_2(H_2O)_4(NO_3)_2(TMeQ[6])_2]^{4+}$ unit, 4 nitrate anions and 26 guest water molecules. It should

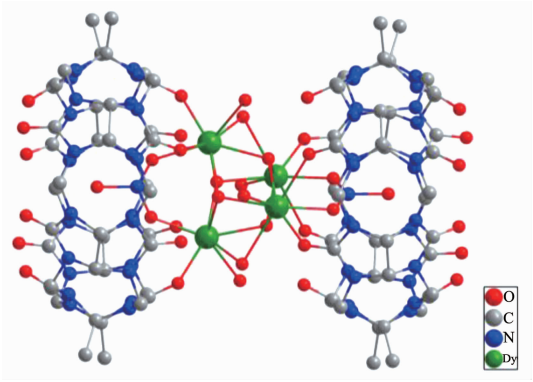

Hydrogen atoms are omitted for clarity

Fig.2 Crystal structure of $[Dy_4(\mu_3\text{-}OH)_4(\mu_2\text{-}OH)_2(H_2O)_4(NO_3)_2(TMeQ[6])_2]^{4+}$ units in **1**

be noted that all dysprosium ions and μ_3-OH atoms have an occupancy factor of 50%, owing to positional disorder, similar to that reported disordered Ln cluster cores[16a-b].

The cationic cluster of **1** has a distorted cubane-shaped core of $[Dy_4(\mu_3\text{-}OH)_4]^{8+}$. Four Dy atoms form a nearly perfect tetrahedron. Two opposite edges of the tetrahedron are further bridged by two μ_2-OH anions, while another two opposite edges are bridged by two NO_3^- anions (Fig.3a). This $[Dy_4(\mu_3\text{-}OH)_4]^{8+}$ cubane cluster core is sandwiched by two TMeQ[6] macrocycles displaying an antiparallel orientation. As shown in Fig.3b, each of Dy ion locates in the center of a square antiprism geometry and is octa-coordinated with contributions from three μ_3-OH, one μ_2-OH anion, two O atoms from a TMeQ[6] ligand, one O atom from nitrate anion, and one terminal aqua ligands. The bond lengths of Dy-O rang from 0.195 4(12) to 0.271 8(9) nm (Table S1), comparable to those in the reported complexes containing the same $[Dy_4(\mu_3\text{-}OH)_4]^{8+}$ core[10-11,17b]. The Dy-$O_{hydroxy}$-Dy angles in the $[Dy_4(\mu_3\text{-}OH)_4]^{8+}$ cubane of **1** are in the range of 99.8(5)°~113.6(7)° obviously larger than 99°[10c].

Complex **2** is isomorphic to **1**. The bond lengths of Tb-O range from 0.210 0(5) to 0.269 0(4) nm and the angles of Tb-$O_{hydroxy}$-Tb range from 99.7(2)° to 113.5(4)° (Table S2), comparable to those in reported Tb complex[24b,26].

2.3 TG analysis

The thermogravimetric (TG) curve of the two complexes under N_2 atmosphere are shown in Fig.4. 1 exhibits the first weight loss of 12% in the temperature range from 24 to 125 ℃, corresponding to the weight loss of 26 lattice water molecules in **1** (Calculated weight loss 12%), and the second weight loss of 2% in the temperature range from 125 to 335 ℃ corresponding to the loss of four coordination water molecules in **1** (Calculated weight loss 2%), and then the metal-organic complex starts to decompose accompanying loss of organic ligands. The TGA curve of complex **2** is similar to that of complex **1**, the first and second weight loss of complex **2** are 12% (Calcd. 12%) and 2%(Calcd. 2%), corresponding to the weight loss of 26 lattice water molecules and 4 coordination water molecules, respectively. The simulated and experimental PXRD patterns for complex **1** and **2** are

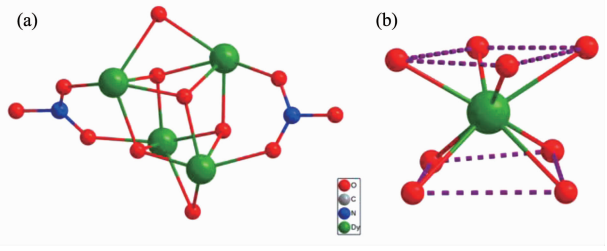

Fig.3 (a) Structure of the $[Dy_4(\mu_3\text{-}OH)_4(\mu_2\text{-}OH)_2(NO_3)_2]^{4+}$ core unit of **1**; (b) the coordination geometry of Dy ion in **1**

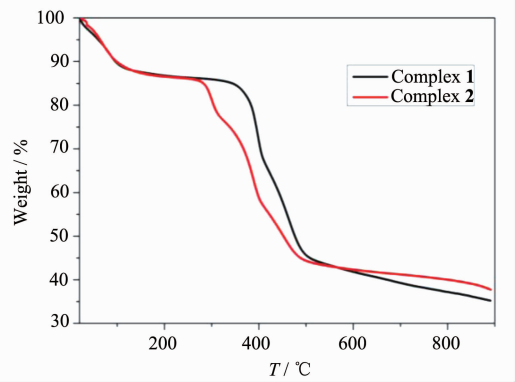

Fig.4　Thermogram of **1** and **2** showing TGA at the heating rate of 10 ℃·min^{-1}

are almost identical as indicated in Fig.S10 and Fig. S11.

2.4　Magnetic properties

The temperature dependence of direct-current (dc) magnetic susceptibility of crushed crystalline sample of **1** and **2** were carried out in an applied magnetic field of 1 000 Oe in the temperature range of 2~300 K. As shown in Fig.5, the observed $\chi_M T$ value of **1** is 55.78 cm^3·mol^{-1}·K at 300 K, close to the expected value of 56.68 cm^3·mol^{-1}·K for four uncoupled Dy^{3+} ions (S=5/2, L=5, $^6H_{15/2}$, g=4/3). The $\chi_M T$ gradually decreases until 50 K and then quickly decreases to a minimum of 36.35 cm^3·mol^{-1}·K at 2 K, which is lower than four times the $\chi_M T$ value of an isolated mononuclear Dy complex at 2 K, suggesting antiferromagnetic coupling between Dy^{3+} ion. Thus the decrease in $\chi_M T$ with decreasing temperature is probably ascribed to a combination of the antiferromagnetic interaction between the Dy^{3+} ions and the thermal depopulation of excited Stark sublevels[27]. The

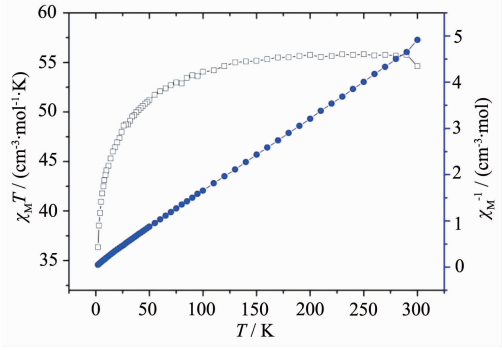

Fig.5　Plots of temperature dependence of $\chi_M T$ vs T and χ_M^{-1} vs T for **1**

data in the range of 30~300 K can be fitted to the Curie-Weiss law, yielding C=63.69 cm^3·mol^{-1}·K and θ=−5.01 K for **1**.

The field dependence of magnetization of **1** is shown in Fig.6. The magnetization at 2 K increases rapidly below 1.5 T, and then slowly and linearly increases without complete saturation up to 7 T. The maximum value for M is 23.08μ_B at 7 T, which is slightly larger than the calculated value for four uncorrelated Dy^{3+} magnetic moments ($4\times5.23\mu_B$) [10]. Indeed, the values are lower than the expected saturation value of 40μ_B (10μ_B for each Dy^{3+} ion for J= 15/2 and g=4/3)[10c-10d], which suggests the presence of a significant anisotropy and low-lying excited states, consistent with the observed nonsuperposition M vs H/T plots at different magnetic fields (Fig.6)[9].

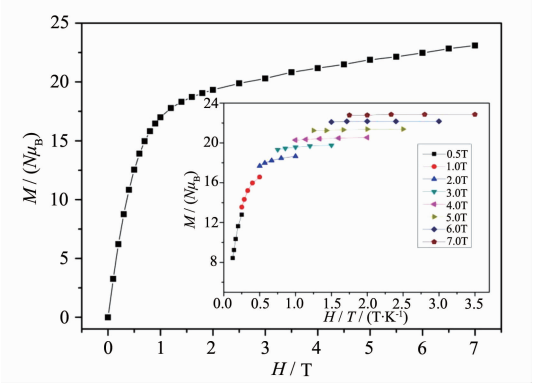

Fig.6　M vs H/T plots for **1** measured in different fields below 7 T

To probe the dynamics of magnetization for **1**, the temperature dependence of ac magnetic susceptibility under H_{dc}=0 Oe and H_{ac}=3 Oe was characterized at the indicated frequencies (1~1500 Hz). As shown in Fig.7, complex **1** displays an obvious frequency dependent out-of-phase signal, indicating the slow relaxation of the magnetization. However, the energy barrier cannot be derived by fitting the peak temperatures to an Arrhenius type expression due to the absence of maxima of out-of-phase susceptibility signals above 2.0 K (Fig.S5). However, the E_a and τ_0 values can be obtained from fitting the ac susceptibility data by adopting Debye model and using the relationship ln (χ''/χ')=lnτ_0+E_a/($K_B T$), if it is assumed that there is only one characteristic relaxation

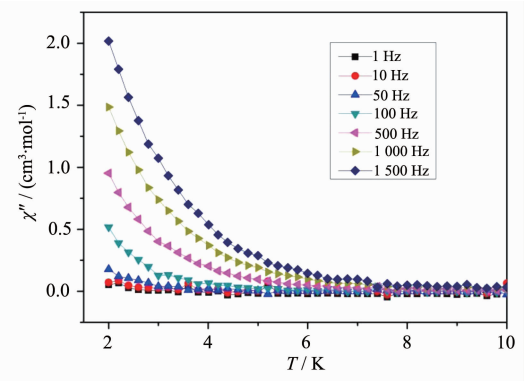

Fig.7 Temperature dependence of the out-of-phase ac susceptibilities at the indicated frequencies for **1** under zero dc field

process[28]. The obtained E_a=35.4 K, τ_0=1.5×10^{-5} s (Fig. 8) are in agreement with the observed values for some other Dy_4 SMMs. For **1**, the slow magnetic relaxation may result from a coupled system involving the four Dy (III) and the magnetic exchange coupling, although the interactions are expected to be very weak.

The $\chi_M T$ value of **2** is 45.66 cm^3·mol^{-1}·K at 300 K (Fig.S4), which is slightly lower than the expected value of 47.28 cm^3·mol^{-1}·K for four uncoupled Tb^{3+} ions (S=3, L=3,$^7F_6$, g=3/2). Similar to **1**, a steady decrease of the $\chi_M T$ values of **2** is observed with deceasing temperature down to 50 K, and then decrease dramatically to 33.05 cm^3·mol^{-1}·K at 2 K. The data from 30 to 300 K are fitted to the Curie-Weiss law, leading to C=44.52 cm^3·mol^{-1}·K and θ=–5.80 K. As shown in Fig.S6, the magnetization increases rapidly below 1.5 T at 2 K, and then slowly and linearly increases to 18.91μ_B at 7 T. Notably, the ac susceptibility results of 2 show that no

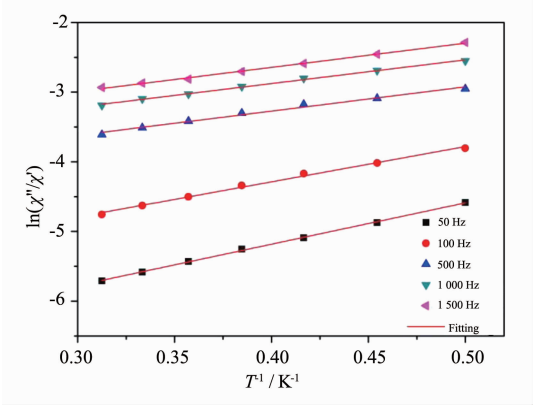

Solid line represents the fitting results over the range of 2.0~3.0 K

Fig.8 Plots of natural logarithm of χ''/χ' vs 1/T for **1**

frequency dependent out-of-phase signal is observed in the region of 2~10 K (Fig.S7). Although Dy^{3+} and Tb^{3+} ions have large spin and high anisotropy, only the Dy_4 cluster exhibits slow paramagnetic relaxation, which may be ascribed to the spin parity effect[26a,29].

2.5 Luminescent properties

The solid-state luminescence of complex **2** at room temperature is shown in Fig.9. Complex **2** exhibits intense photoluminescence upon excitation at 375 nm. The emission spectrum of **2** can be ascribed to the characteristic $^5D_4 \rightarrow {}^7F_J$ transitions (J=6, 5, 4, 3). The most intense peak with its maximum at 546 nm is attributed to the $^5D_4 \rightarrow {}^7F_5$ transition. Besides this main emission line, the second intense peak at 492 nm (J=6), and much less intense two peaks at 588 nm (J=4) and 622 nm (J=3), respectively, are also observed. This means that TMeQ[6] ligand exhibits efficient energy transfer to Tb^{3+} ion. When excited at 265 nm in the solid state at room temperature, compound **1** displays a wide luminescence spectrum with emission maximum at 390 nm (Fig.S8), which can be assigned to ligand fluorescence (Fig.S9). Compared with the emission of the free ligand at 378 nm, the red shift in **1** may be ascribed to the increase of ligand conformational rigidity.

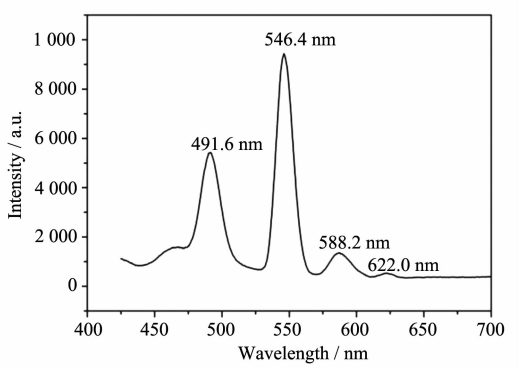

Fig.9 Emission spectrum of **2** under 375 nm excitation in the solid state at room temperature

3 Conclusions

In summary, two TMeQ[6]-supported lanthanide sandwich complexes containing a cubane-like $[Ln_4(\mu_3\text{-}OH)_4]^{8+}$ cluster core were prepared and characterized. Magnetic studies reveal that Dy_4 exhibits slow

magnetic relaxation behavior. While the Tb^{3+} analogue of $[Ln_4(\mu_3\text{-}OH)_4]^{8+}$ cluster core displays interesting luminescent property. The present work not only affords the first example of TMeQ[6] supported lanthanide hydroxide cluster with slow magnetic relaxation behavior, but also provides a new synthetic approach to prepare new lanthanide SMMs based on Cucurbit[*n*] urils.

Supporting information is available at http://www.wjhxxb.cn

References:

[1] Troiani F, Affronte M. *Chem. Soc. Rev.*, **2011**,**40**:3119-3129

[2] Rogez G, Donnio B, Terazzi E, et al. *Adv. Mater.*, **2009**,**21**:4323-4333

[3] (a) Sessoli R, Gatteschi D, Caneschi A, et al. *Nature*, **1993**, **365**:141-143
(b) Benelli C, Gatteschi D. *Chem. Rev.*, **2002**,**102**:2369-2387
(c) Bagai R, Christou G. *Chem. Soc. Rev.*, **2009**,**38**:1011-1026
(d) Kostakis G E, Akoab A M, Powell A K. *Chem. Soc. Rev.*, **2010**,**39**:2238-2271

[4] (a) Coronado E, Day P. *Chem. Rev.*, **2004**,**104**:5419-5448
(b) Sanvito S. *Chem. Soc. Rev.*, **2011**,**40**:3336-3355

[5] Sokol J J, Hee A G, Long J R. *J. Am. Chem. Soc.*, **2002**, **124**:7656-7657

[6] Sessoli R, Tsai H L, Schake A R, et al. *J. Am. Chem. Soc.*, **1993**,**115**:1804-1816

[7] Murrie M. *Chem. Soc. Rev.*, **2010**,**39**:1986-1995

[8] (a) Woodruff D N, Winpenny R E P, Layfield R A. *Chem. Rev.*, **2013**,**113**:5110-5148
(b) Hewitt I J. Tang J K, Madhu N T, et al. *Angew. Chem. Int. Ed.*, **2010**,**49**:6352-6356
(c) Guo Y N, Xu G F, Gamez P, et al. *J. Am. Chem. Soc.*, **2010**,**132**:8538-8539

[9] Bi Y F, Wang X T, Liao W P, et al. *Inorg. Chem.*, **2009**,**48**:11743-11747

[10](a) Abbas G, Lan Y H, Kostakis G E, et al. *Inorg. Chem.*, **2010**,**49**:8067-8072
(b) Lin P H, Burchell T J, Ungur L, et al. *Angew. Chem. Int. Ed.*, **2009**,**48**:9489-9492
(c) Ke H S, Gamez P, Zhao L, et al. *Inorg. Chem.*, **2010**,**49**:7549-7557
(d) Tang J K, Hewitt I, Madhu N T, et al. *Angew. Chem. Int. Ed.*, **2006**,**45**:1729-1733

[11]Kong X J, Wu Y L, Long L S, et al. *J. Am. Chem. Soc.*, **2009**,**131**:6918-6919

[12]Wang R, Selby H D, Liu H, et al. *Inorg. Chem.*, **2002**,**41**:278-286

[13]Deacon G B, Feng T, Hockless D C R, et al. *Chem. Commun.*, **1997**:341-342

[14]Peng J B, Kong X J, Zhang Q C, et al. *J. Am. Chem. Soc.*, **2014**,**136**:17938-17941

[15]Bürgstein M R, Gamer M T, Roesky P W, et al. *J. Am. Chem. Soc.*, **2004**,**126**:5213-5218

[16]Liu C M, Zhang D Q, Hao X, et al. *Cryst. Growth Des.*, **2012**,**12**:2948-2954

[17](a) Hewitt I J, Lan Y, Anson C E, et al. *Chem. Commun.*, **2009**:6765-6767
(b) Gao Y, Xu G F, Zhao L, et al. *Inorg. Chem.*, **2010**,**48**:11495-11497
(c) Habib F, Lin P O, Long J, et al. *J. Am. Chem. Soc.*, **2011**,**133**:8830-8833

[18](a) Behrend R, Meyer E, Rusche F. *Justus Liebigs Ann. Chem.*, **1905**,**339**:1-37
(b) Freeman W A, Mock W L, Shih N Y. *J. Am. Chem. Soc.*, **1981**,**103**:7367-7368
(d) Day A I, Blanch R J, Arnold A, et al. *Angew. Chem.*, Int. Ed., **2002**,**41**:275-277

[19](a) Flinn A, Hough G C, Stoddart J F, et al. *Angew. Chem. Int. Ed.*, **1992**,**31**:1475-1477
(b) Zhao J Z, Kim H J, Oh J, et al. *Angew. Chem., Int. Ed.*, **2001**,**40**:4233-4235
(c) Jon S Y, Selvapalam N, Oh D H. et al. *J. Am. Chem. Soc.*, **2003**,**125**:10186-10187
(d) Huang W H, Zavalij P Y, Isaacs L. *Angew. Chem. Int. Ed.*, **2007**,**119**:7569-7571
(e) Zhao Y J, Xue S F, Zhu Q J, et al. *Chin. Sci. Bull.*, **2004**,**49**:1111-1116

[20]Chen W J, Yu D H, Xiao X, et al. *Inorg. Chem.*, **2011**,**50**:6956-6964

[21](a) Hernandez-Molina R, Sokolov M N, Sykes A G. *Acc. Chem. Res.*, **2001**,**34**:223-230
(b) Fedin V P. *J. Coord. Chem.*, **2004**,**30**:151-152
(c) Hernandez-Molina R, Sokolov M N, Clausen M, et al. *Inorg. Chem.*, **2006**,**45**:10567-10575
(d) Gushchin A L, Ooi B, Harris P, et al. *Inorg. Chem.*, **2009**,**48**:3832-3839

[22](a) Lü J, Lin J X, Cao M N, et al. *Coord. Chem. Rev.*, **2013**, **257**:1334-1357
(b) Ni X L, Xue S F, Tao Z. *Coord. Chem. Rev.*, **2015**,**287**:

89-113

[23](a) Tripolskaya A A, Mainicheva E A, Mitkina T V, et al. *Russ. J. Coord. Chem.*, **2005**,**31**:768-774

(b) Thuery P. *Inorg. Chem.*, **2009**,**48**:4497-4513

(c) Thuery P. *Inorg. Chem.*, **2010**,**49**:9078-9085

(d) Thuery P. *Inorg. Chem.*, **2011**,**50**:10558-10560

(e) Kushwaha S, Rao S A, Sudhakar P P. *Inorg. Chem.*, **2012**,**51**:267-273

(f) Liang L L, Ni X L, Zhao Y, et al. *Inorg. Chem.*, **2013**, **52**:1909-1915

(g) Liang L L, Zhao Y, Tao Z, et al. *CrystEngComm*, **2013**, **15**:3943-3950

(h) Liu J X, Hu Y F, Lin R L, et al. *CrystEngComm*, **2012**, **14**:6983-6989

[24](a) Gerasko O A, Mainicheva E A, Naumova M I, et al. *Inorg. Chem.*, **2008**,**47**:8869-8880

(b) Gerasko O A, Mainicheva E A, Naumova M I, et al. *Eur. J. Inorg. Chem.*, **2008**,**3**:416-424

[25]*SHELXTL Program Package*, *Version* 6.10, Bruker AXS, Inc., Madison, WI, **2000**.

[26](a) Yan P F, Lin P H, Habib F. et al. *Inorg. Chem.*, **2011**, **50**:7059-7065

(b) Jami A K, Baskar V, Sanudo E C, et al. *Inorg. Chem.*, **2013**,**52**:2432-2438

[27]Langley S K, Moubaraki B, Forsyth C M, et al. *Dalton Trans.*, **2010**,**39**:1705-1708

[28]Bartolomé J, Filoti G, Kuncser V, et al. *Phys. Rev. B*, **2009**, **80**:014430

[29](a) Wernsdorfer W, Bhaduri S, Boskovic C, et al. *Phys. Rev. B*, **2002**,**65**:180403

(b) Wernsdorfer W, Chakov N E, Christou G, et al. *Phys. Rev. Lett.*, **2005**,**95**:037203